IET Power Electronics

Research Article

Decentralised non-linear *I–V* droop control to improve current sharing and voltage restoration in DCNG clusters

ISSN 1755-4535
Received on 26th February 2019
Revised 29th September 2019
Accepted on 21st October 2019
E-First on 8th November 2019
doi: 10.1049/iet-pel.2019.0263
www.ietdl.org

Mahdi Mosayebi[1], Seyed Mohammad Sadeghzadeh[1] ✉, Mohammad Hassan Khooban[2], Josep M. Guerrero[3]

[1]Faculty of Engineering, Shahed University, Tehran, Iran
[2]Department of Engineering, Aarhus University, 8200 Aarhus, Denmark
[3]Department of Energy Technology, Aalborg University, Aalborg, Denmark
✉ *E-mail: Sadeghzadeh@shahed.ac.ir*

Abstract: This study proposes a new decentralised non-linear *I–V* droop control to achieve current sharing and voltage restoration for paralleled DC nanogrids (DCNGs) in a cluster. The performance of the conventional droop methods in current sharing among parallel converters degrades due to line impedances. The proposed method improves current sharing among the DCNGs with parallel-connected converters by considering the effect of line impedance, which is an important issue in practical applications. By the proposed method, desired current sharing from the light-load to heavy-load condition is achieved. Since only local information (the output voltage and output current of the DCNGs) is used, the proposed method is fully decentralised, and no communication infrastructure is required, which improves the reliability and stability of the overall system. Furthermore, Lyapunov stability theory is applied to investigate the stability of the proposed method. Additionally, the plug-and-play feature is achieved as an important desired functionality in the DCNGs as well as the proposed method provides scalability and modularity for the DCNGs in a cluster. In the end, theoretical analysis and experimental results validate the effectiveness of the proposed control framework for different scenarios.

1 Introduction

By utilising renewable energy sources (RESs) and energy storage systems (ESSs), the concept of the DC microgrids (DCMGs) has been introduced for more reliability, power quality, efficiency, and environmental concerns [1]. Recently, the DCMGs have gained more popularity due to the benefits such as the absence of reactive power and harmonic issues, simplicity in control, and higher efficiency in comparison with the AC microgrids. Moreover, intrinsic DC voltage and current output of the RESs and ESSs enhanced the efficiency in the DCMGs due to fewer number of power conversions, respectively. Similarly, the growth of DC loads and end-user appliances such as computers and light-emitting diodes caused more attention to the DCMGs [2]. However, by the interconnection of multiple DC nanogrids (DCNGs) based on the number of loads, low-power DCNGs clusters have been introduced [3]. As shown in Fig. 1, in the DCNGs structure, RESs and ESSs are connected to the load or DC bus through DC–DC power electronic converters. To have more flexibility and stability during several loading conditions, the parallel operation of the DCNGs in a cluster is preferred [4].

With paralleling of several converters in a cluster, current-sharing issues are appearing. To have proper current sharing and voltage regulation in the DCNGs cluster, several control strategies have been proposed in the literature. On the basis of well-defined structure control in [5], three-level hierarchical controls have been presented known as primary, secondary, and tertiary control levels. Primary control generally follows the set points given by the secondary control level to perform the control of power, voltage, and current, locally. Secondary control generates the reference values of current and voltage on the top of the primary control. This control level is responsible for the power quality, synchronisation of microgrid, coordination among RESs and ESSs, and so on. Finally, tertiary control is used for optimisation and management in the overall system [6]. To have a proper performance in secondary and tertiary control levels, a communication structure has been developed for sharing data between agents in the DCNG cluster, which lead to coordinated control among the DCNGs. On the basis of the structure of communication links, centralised and distributed controls have been presented to achieve voltage regulation, current sharing, and power management in the DCNG cluster [7–9].

In another classification, DCNGs control strategies can be generally categorised into two main structures known as master–slave and droop control [10]. Master–slave scheme suffers from the single point of failure, which means the operation of the whole of DCNG depends on the operation of the master agent in a cluster [11]. To overcome the above drawback, the droop control method has been adopted in several studies in primary control level, which improves the reliability of the DCNG cluster [12–14]. Meanwhile, by implementing a conventional droop control method, the voltage reference linearly increased when the output current decreases by using a virtual resistance and it is evident that the output voltage deviates from the nominal value. Moreover, to have a proper current sharing in paralleled converter with a conventional droop control method, the virtual resistance should be adopted large, but large virtual resistance causes more deviation in the voltage [12].

To improve the accuracy of the current sharing in a DCNG cluster, several control schemes based on adaptive droop control have been presented [15]. In [16], a state-of-charge (SOC)-based adaptive droop control is proposed, which adaptively changes the droop gains to achieve current sharing between paralleled converters. To improve the transient current sharing among the DCNGs, Dragicevic *et al.* [17] suggested an adaptive droop control based on the SOC. However, in these methods, the effect of the line impedance is not considered.

In [18–20], droop control methods based on the communication link are proposed. In [21], the average current sharing is proposed, in which the average current is calculated with global measurement in a cluster. To achieve current sharing and voltage restoration simultaneously, master–slave, centralised [6], and distributed controllers in secondary and tertiary control levels are proposed in [22]. The method in [7] tries to enhance the current sharing among the paralleled DCNGs and restore voltage in nominal value. However, these strategies require a communication network for an appropriate operation, which affects the reliability of the system and increases the cost of implementing the system.

In a new paradigm, the non-communication decentralised droop control schemes are proposed, which are easier to implement. To achieve current sharing in a decentralised manner in [23], an adaptive droop control based on the superimposed frequency is proposed. In this method, due to the superimposed small AC voltage, the power quality of the system degrades with oscillations in voltage and current. Moreover, in [23–25], several decentralised droop control methods are proposed to improve the current sharing among the DCNGs in a cluster. They also present high reliability, plug-and-play feature, and modularity. However, in these methods, the effect of line impedance has not been considered. Moreover, in [26], a non-linear *V–I* droop control is proposed to achieve current sharing and voltage restoration. However, Wang *et al.* [25], without the consideration of the line impedance, showed that the *I–V* droop control method represents faster dynamics comparing with the *V–I* droop control, which is better to use in current sharing among the DCNGs in a cluster.

Therefore, to rectify these limitations of the aforementioned strategies, in this paper, a novel decentralised non-linear *I–V* droop control is proposed, which considers the effect of the line impedance. In the proposed method, the current sharing and voltage restoration among the DCNGs in a cluster enhance by adjusting the proper droop gain based on the local measuring of the output voltage and output current of each DCNG. The major novelties of the proposed method are: (i) accurate current sharing among the DCNGs in light and heavy-loading conditions with different line impedance; (ii) only local information is used and no communication is needed due to the fully decentralised control method; (iii) plug-and-play capability is achieved in the case of the connection and disconnection of the DCNGs; and (iv) regulation voltage is guaranteed in an acceptable range.

The remaining part of this paper is organised as follows: the modelling of the DCNGs is provided in Section 2. In Section 3, the current sharing between two DCNGs is reviewed. In Section 4, the proposed non-linear *I–V* droop control is introduced. Section 5 includes the stability analysis of the system. In Section 6, the experimental results are presented. Finally, this paper is concluded in Section 7.

2 Modelling of the DCNGs

As illustrated in Fig. 1, in the islanded DCNG cluster, several parallel DCNGs including the photovoltaic (PV) systems and ESSs are connected to the DC bus, which are controlled with droop control to achieve power sharing among DCNGs. In the following, each of the PV systems and ESSs in the DCNG are further investigated.

2.1 PVs systems

PV systems can convert the solar energy to electrical energy directly. The electrical characteristic of the PVs array can be expressed as [20]

$$I_{\rm PV} = N_{\rm p} I_{\rm ph} - N_{\rm p} I_{\rm rs}\left(\exp\left(\frac{qV_{\rm PV}}{kT_{\rm T}A_{\rm IF}N_{\rm s}N_{\rm c}}\right) - 1\right) \tag{1}$$

where $I_{\rm PV}$ and $V_{\rm PV}$ are the current and voltage of the PV system, respectively; $N_{\rm s}$ and $N_{\rm p}$ are the number of the series-connected modules per string and parallel string, respectively; $I_{\rm ph}$ is the short-circuit current of the one string; $I_{\rm rs}$ is the diode reverse saturation current; $N_{\rm c}$ is the number of the series cells per module; k is the Boltzman's constant; q is the unit electric charge; $T_{\rm T}$ is the P–N junction temperature in Kelvin; and $A_{\rm IF}$ is the ideality factor. The PV temperature characteristic can be considered as a function of the ambient temperature and the solar irradiation as follows:

$$\frac{{\rm d}T_{\rm T}}{{\rm d}t} = \frac{1}{C_{\rm PV}}\left(k_{\rm in,\,PV}\phi - \frac{V_{\rm PV}I_{\rm PV}}{A_{\rm PV}} - k_{\rm loss}(T_{\rm c} - T_{\rm a})\right) \tag{2}$$

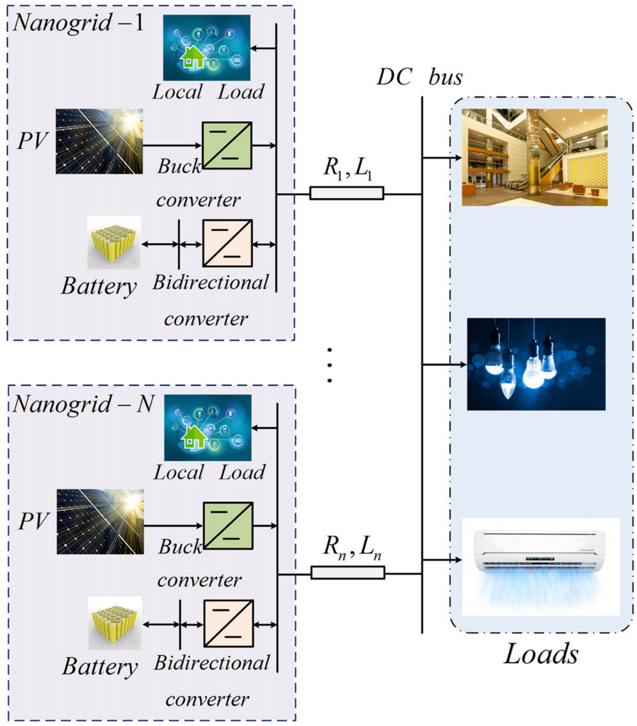

Fig. 1 *Parallel DCNGs in a cluster*

According to the DC bus voltage and output voltage of the PVs, the PVs are connected to the DC bus via boost or buck converters.

2.2 Battery ESS

Utilisation of the ESSs such as lithium-ion batteries in the DCNG can improve the reliability and efficiency of the islanded DCNG cluster. Battery ESS can be modelled with a controllable voltage source and internal resistance as follows:

$$E = E_0 - \frac{KQ}{Q - \int i\,{\rm d}t} + A\exp\left(-B\int i\,{\rm d}t\right) \tag{3}$$

Moreover, the SOC of the battery can be written as

$${\rm SOC} = 100\left(1 - \frac{1}{Q}\int i\,{\rm d}t\right) \tag{4}$$

where Q is the capacity of the battery. More details of the battery modelling and definition parameters can be found in [21].

As mentioned before, the paralleled DCNGs in the stand-alone DCNG cluster are controlled to achieve proper voltage regulation as well as current sharing among DCNGs. In the following section, to realise this goal, current-sharing issue in the droop-based control methods is presented.

3 Current sharing in droop-based control

In a DCNG cluster, several parallel sources are connected to the DC bus through cables to deliver the power to the loads. With respect to the location of sources and common load, the cables have different lengths in a cluster. On the basis of the current rating of the DCNGs' cable, various cables have different equivalent resistance. Moreover, different length of the cable of each DCNG in a cluster leads to unequal resistance and degrades the current sharing among the DCNGs. To analyse this issue, two parallel DCNGs are considered, which are connected to the common load. The equivalent circuit is shown in Fig. 2*a*, where V_1 and V_2 are the output voltages of the DCNG1 and DCNG2, respectively. R_1 and R_2 are the line resistances between each DCNG to load terminal, respectively. $R_{\rm LOAD}$ is the equivalent resistance of the common load. Let, the designed droop resistances of the DCNG1 and

DCNG2 are R_{d1} and R_{d2}, respectively. The droop law can be written as follows:

$$V_i = V^* - R_{di} I_i \tag{5}$$

where R_{di} and I_i are the droop resistance and current of the ith DCNG, respectively. V^* is the set point voltage and V_i is the output voltage of the ith DCNG. The droop resistance can be defined as

$$R_{di} = \frac{\Delta V}{I_{max}} \tag{6}$$

where ΔV and I_{max} are the desired voltage deviation from reference voltage and maximum output current of the DCNGs, respectively.

Furthermore, the total resistance from the DCNGs to the load can be calculated as follows:

$$R'_{d1} = R_{d1} + R_1 \tag{7}$$

$$R'_{d2} = R_{d2} + R_2 \tag{8}$$

Applying Kirchhoff's laws to the equivalent circuit in Fig. 2*a* yields

$$I_1 = \frac{R_{LOAD}(V_1 - V_2) + V_1 R'_{d2}}{R'_{d1} R'_{d2} + R_{LOAD} R'_{d1} + R_{LOAD} R'_{d2}} \tag{9}$$

$$I_2 = \frac{R_{LOAD}(V_2 - V_1) + V_2 R'_{d1}}{R'_{d1} R'_{d2} + R_{LOAD} R'_{d1} + R_{LOAD} R'_{d2}} \tag{10}$$

where I_1 and I_2 are the output currents of the DCNG1 and DCNG2, respectively. The difference between the currents of the two paralleled DCNGs is given by

$$I_1 - I_2 = \frac{2(V_1 - V_2)}{(R'_{d1}) + (R'_{d2}) + (((R'_{d1})(R'_{d2}))/R_{LOAD})} + \frac{V_1(R'_{d2}) - V_2(R'_{d1})}{(R'_{d1})(R'_{d2}) + (R'_{d1})R_{LOAD} + (R'_{d2})R_{LOAD}} \tag{11}$$

The load current with respect to Fig. 2*a* can be obtained as

$$\begin{cases} V_{bus} = V_1 - I_1 R'_{d1} = V_2 - I_2 R'_{d1} \\ I_{LOAD} = I_1 + I_2 \end{cases} \tag{12}$$

If the set point voltage of two DCNGs is the same, the current sharing will be as below:

$$\frac{I_1}{I_2} = \frac{R_{d2} + R_2}{R_{d1} + R_1} \tag{13}$$

It means that the DCNG with larger line resistance injects less current to the load. As discussed in [26], using droop resistance can improve the current sharing among the DCNGs. From Fig. 2*b*, it can be seen that the high droop gain yields better current sharing. However, high droop gain affects the voltage deviation [12]. Therefore, in the droop control strategy, it is a trade-off between current sharing and voltage regulation. Moreover, the difference of the line resistance, which is inevitable in practical application, affects the current sharing.

To have proper current sharing and good voltage regulation in the droop control, optimisation on the droop resistance trajectory should be considered. For a specified voltage deviation, several droop curves can be considered from no-load to full-load operation of the DCNGs. The curves can be represented by the following equation:

$$V_i = V^* - k_i(I_i^n), \quad n \in R^+ \tag{14}$$

where

$$k_i = \frac{\Delta V}{(I_{i,\max})^n} \tag{15}$$

On the basis of (14), the droop resistance expression can be derived as

$$R_{di} = \frac{dV_i}{dI_i} = n\, k_i (I_i)^{n-1} \tag{16}$$

As shown in Fig. 3, for different values of n, the droop resistance changes from no load to full load. To have a symmetrical operation for a bidirectional converter, the current is considered from −1 to 1. From Fig. 3, it can be seen that when $n > 1$ the value of the droop gain is close to zero under light-loading conditions; moreover, in heavy-loading conditions, the value of the droop gain is higher than the linear droop. For $n = 1$, regardless of the output current of the converter, the droop gain is constant and it is the linear droop method.

It is obvious that linear droop method in heavy-load condition has undesirable performance due to small droop gain and the current sharing is degraded. Moreover, about the non-linear droop methods, this phenomenon is appearing for light-load conditions. Therefore, to have a good performance through all loading conditions, by merging the good features of these methods, a novel non-linear *I–V* droop is presented in the next section of this paper.

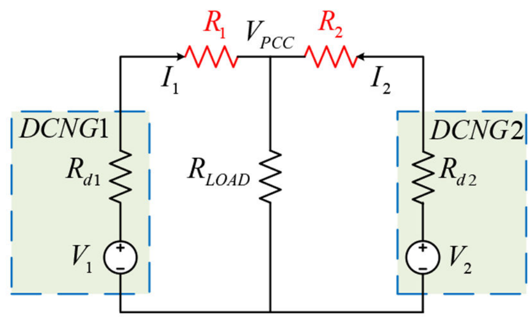

a

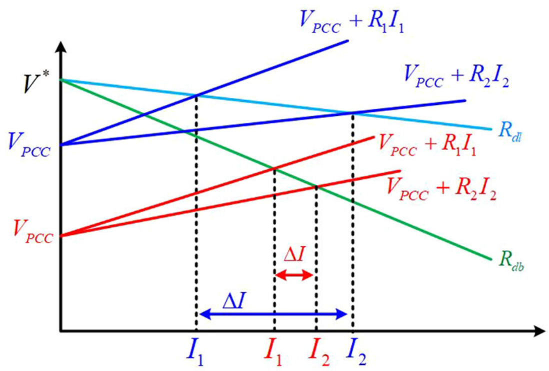

b

Fig. 2 *Equivalent circuit*
(a) Equivalent circuit of two parallel DCNGs, ***(b)*** Effect of different droop gains in conventional droop method

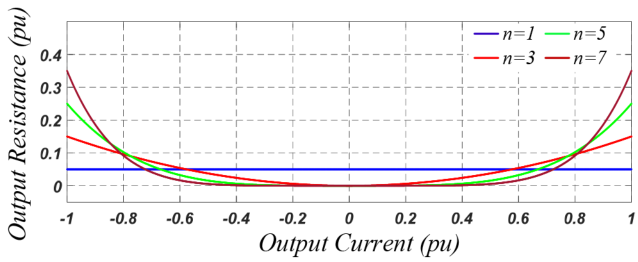

Fig. 3 *Droop gains based on the output current for different values of n*

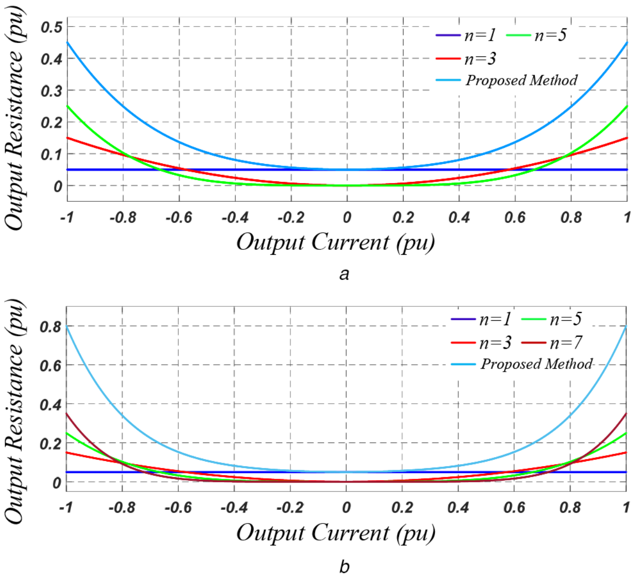

Fig. 4 *Different droop gain based on the proposed method*
(a) For $n = 1, 3, 5$, ***(b)*** For $n = 1, 3, 5, 7$

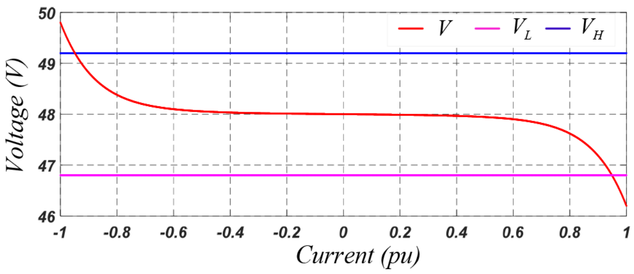

Fig. 5 *Deviation of voltage from no-load to full-load condition*

4 Proposed *I–V* droop control technique

To overcome the limitation of the conventional linear and non-linear methods, and to satisfy good performance in the current sharing and voltage restoration, a novel non-linear *I–V* droop-based control is proposed.

From (5), if the reference output from the droop characteristic is reversed, the *I–V* droop control can be achieved by increasing the current reference when the bus voltage decreases as follows:

$$I_{\text{ref},\,i} = \frac{V^* - V_i}{R_{\text{d}i}} \tag{17}$$

In other words, to obtain a faster dynamic response, a single current proportional–integral control loop is replaced with the dual voltage and current control loops. As shown in [25], the *V–I* dual-loop droop control exhibits slower dynamics in comparison with the *I–V* droop control. By expanding (14), with consideration of the linear droop gain (i.e. n=1), the general equation of the droop curve can be obtained as follows:

$$V_i = V^* - k_1 I_i - k_i I_i^n \tag{18}$$

The selection of n (i.e. $n = 3, 5, 7, \ldots$) is depending on the amount of voltage deviation and the maximum current value in the ith DCNG [27]. It should be noted that to have a symmetrical performance for the bidirectional converter, it is preferred to select the droop curves with odd values. Therefore, (18) can be rewritten as

$$k_1 I_i = V^* - V_i - k_i I_i^n \tag{19}$$

Moreover, finally (19) based on the *I–V* droop (17) can be expressed as

$$I_{\text{ref},\,i} = \frac{V^* - V_i}{k_1} - \left(\frac{k_i}{k_1} I_i^n\right) \tag{20}$$

where k_1 is the linear droop gain and k_i is defined in (15). As depicted in Fig. 4, it can be seen that, based on (20), the proposed droop method has both good features of linear and non-linear droop methods. To put it another way, throughout all loading conditions, the proposed method has maximum available droop gain and satisfies the best current sharing. The compensation current term is subtracted from reference current to adjust the best droop gain in a non-linear manner. Meanwhile, from Fig. 5, it can be seen that the voltage deviation from the reference value in full load is more than the expected deviation (i.e. $V_{\text{H}} = 49.2\,\text{V}$ and $V_{\text{L}} = 46.8\,\text{V}$) [27]. To improve this deviation, a voltage compensation method based on the amount of line resistance is proposed. In this method, the voltage compensation term is added to the reference voltage with respect to the line resistance. The modified droop method equation can be written as follows:

$$I_{\text{ref},\,i} = \frac{V^* - V_i + \Delta V_i}{k_1} - \left(\frac{k_i}{k_1} I_i^n\right) \tag{21}$$

In (21), I_i and V_i are the output current and output voltage of the DCNG. The proposed method in (21) overcomes the drawback voltage deviation from the acceptable range. Moreover, since only the local information is used, the proposed method is fully decentralised and no communication infrastructure is needed. The overall proposed control scheme is shown in Fig. 6.

It should be noted that in case of the different power ratings of the DCNGs, the values of k_i can be modified based on the rating of other DCNGs [26].

5 Stability analysis of the proposed method

To analyse the effect of line impedance in the stability of the system and to investigate the performance of the proposed method, a detailed stability analysis is carried out based on the Lyapunov approach.

5.1 Modelling of the proposed method

As shown in Fig. 6, the droop equation can be written as

$$I_{\text{ref},\,i} = k_1^{-1}(V^* - V_{\text{C},\,i} + \Delta V_i - (k_i I_{\text{o},\,i}^n)) \tag{22}$$

To investigate the stability of the system based on the Lyapunov approach, n-paralleled DCNG in a cluster is considered. Fig. 7 shows the model of the DCNG connected to the DCMG network. Therefore, (22) can be rewritten in matrix form as

$$\boldsymbol{I}_{\text{ref}} = \boldsymbol{k}_1^{-1}(\boldsymbol{V}^* - \boldsymbol{V}_{\text{C}} + \boldsymbol{R}\,\boldsymbol{I}_{\text{o}} - (\boldsymbol{k}_i \boldsymbol{I}_{\text{o}}^n)) \tag{23}$$

where

$$\boldsymbol{I}_{\text{o}} = [I_{\text{o}1} \quad \cdots \quad I_{\text{o}n}]^{\text{T}}$$

$$\boldsymbol{I}_{\text{ref}} = [I_{\text{ref},\,1} \quad \cdots \quad I_{\text{ref},\,n}]^{\text{T}}$$

$$\boldsymbol{k}_1 = \text{diag}\left([k_{1,\,1} \quad \cdots \quad k_{1,\,n}]^{\text{T}}\right)$$

$$\boldsymbol{V}^* = 1_{\boldsymbol{n}} V^*$$

$$\boldsymbol{k}_i = \text{diag}\left([k_{i,\,1} \quad \cdots \quad k_{i,\,n}]^{\text{T}}\right)$$

$$\boldsymbol{R} = \text{diag}\left([R_1 \quad \cdots \quad R_n]^{\text{T}}\right)$$

Equation (23) can be rewritten as follows:

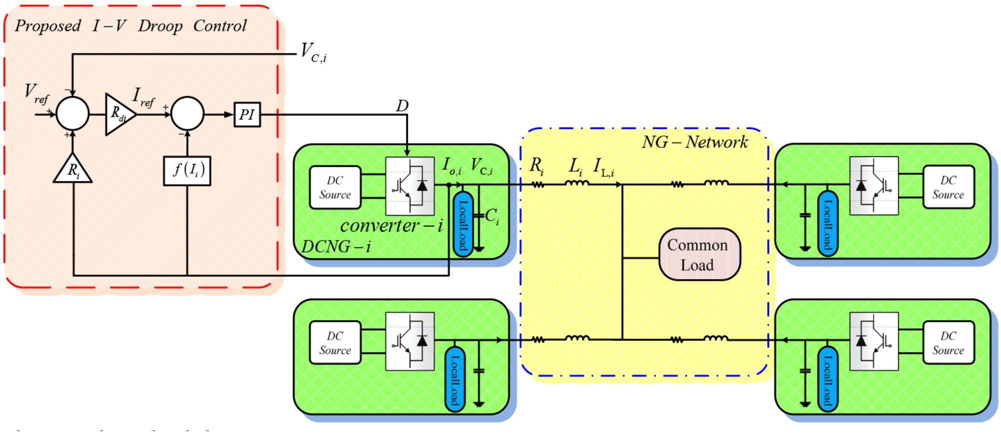

Fig. 6 *Proposed control method diagram*

$$\begin{aligned}\boldsymbol{I}_{\text{ref}} = {} & \boldsymbol{k}_1^{-1}\boldsymbol{V}^* \\ & -\boldsymbol{k}_1^{-1}\boldsymbol{V}_{\text{C}} \\ & -\boldsymbol{k}_1^{-1}\left(-\boldsymbol{R}\,\boldsymbol{I}_{\text{o}} + (\boldsymbol{k}_i\boldsymbol{I}_{\text{o}}^n)\right)\end{aligned} \tag{24}$$

Here, the dynamics of the converter are modelled as a first-order system for the simplification of the analysis [5]. Therefore, the relationship between $I_{\text{ref},\,i}$ and I_{oi} can be written as

$$I_{oi} = \frac{1}{\tau s + 1} I_{\text{ref},\,i} \tag{25}$$

where τ is the equivalent control bandwidth for the converter. Equation (25) can be presented in matrix form as

$$\dot{\boldsymbol{I}}_{\text{o}} = \Gamma(\boldsymbol{I}_{\text{ref}} - \boldsymbol{I}_{\text{o}}) \tag{26}$$

where $\Gamma = (1/\tau I_n)$.

Substituting (24) into (26) yields

$$\dot{\boldsymbol{I}}_{\text{o}} = \Gamma\left(\boldsymbol{k}_1^{-1}\boldsymbol{V}^* - \boldsymbol{k}_1^{-1}\boldsymbol{V}_{\text{C}} - \boldsymbol{k}_1^{-1}\left(-\boldsymbol{R}\,\boldsymbol{I}_{\text{o}} + (\boldsymbol{k}_i\boldsymbol{I}_{\text{o}}^n)\right) - \boldsymbol{I}_{\text{o}}\right) \tag{27}$$

Equation (27) can be rewritten as follows:

$$\begin{aligned}\dot{\boldsymbol{I}}_{\text{o}} = {} & \Gamma\left(\boldsymbol{k}_1^{-1}\right)\boldsymbol{V}^* \\ & -\Gamma\left(\boldsymbol{k}_1^{-1}\right)\boldsymbol{V}_{\text{C}} \\ & -\Gamma\left(\boldsymbol{k}_1^{-1}\left(-\boldsymbol{R} + \left(\boldsymbol{k}_i\boldsymbol{I}_{\text{o}}^{n-1}\right)\right) + \boldsymbol{I}_n\right)\boldsymbol{I}_{\text{o}}\end{aligned} \tag{28}$$

Furthermore, the relationship between the output current of each DCNG I_{oi}, capacitor voltage $V_{\text{C},\,i}$, and output current for the line $I_{\text{L}i}$ can be expressed as

$$\dot{V}_{\text{C},\,i} = \frac{1}{C_i}(I_{oi} - I_{\text{L}i}) \tag{29}$$

Equation (29) in matrix form can be defined as

$$\dot{\boldsymbol{V}}_{\text{C}} = \boldsymbol{C}^{-1}(\boldsymbol{I}_{\text{o}} - \boldsymbol{I}_{\text{L}}) \tag{30}$$

Additionally, Han *et al.* [28] showed that in a cluster of microgrids with any topology, the relationship between output capacitor voltage in each DCNG ($V_{\text{C},\,i}$) and the line current ($I_{\text{L}i}$) can be modelled in one matrix called $\boldsymbol{L}_{\text{L}}$ in this work. Therefore, (30) can be rewritten as follows:

$$\dot{\boldsymbol{V}}_{\text{C}} = \boldsymbol{C}^{-1}(\boldsymbol{I}_{\text{o}} - \boldsymbol{L}_{\text{L}}\,\boldsymbol{V}_{\text{C}}) \tag{31}$$

Considering (27) and (30), the overall system can be described as

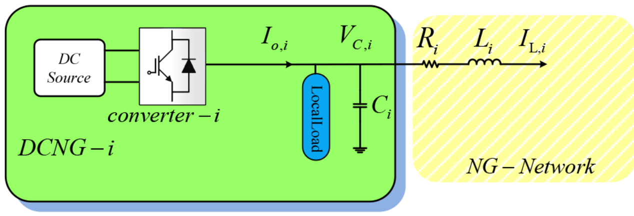

Fig. 7 *Model of DCNG for stability analysis*

$$\begin{bmatrix}\dot{\boldsymbol{V}}_{\text{C}} \\ \dot{\boldsymbol{I}}_{\text{o}}\end{bmatrix} = \begin{bmatrix} -\boldsymbol{C}^{-1}\boldsymbol{L}_{\text{L}} & \boldsymbol{C}^{-1} \\ -\Gamma\cdot\boldsymbol{k}_1^{-1} & -\Gamma\left(\boldsymbol{k}_1^{-1}\left(-\boldsymbol{R} + \left(\boldsymbol{k}_i\boldsymbol{I}_{\text{o}}^{n-1}\right)\right) + \boldsymbol{I}_n\right)\end{bmatrix}\begin{bmatrix}\boldsymbol{V}_{\text{C}} \\ \boldsymbol{I}_{\text{o}}\end{bmatrix} + \begin{bmatrix}0 \\ \Gamma\,\boldsymbol{k}_1^{-1}\end{bmatrix}\boldsymbol{V}^* \tag{32}$$

5.2 Stability evaluation based on the Lyapunov approach

To develop the stability analysis of the proposed method based on the Lyapunov approach, a positive definite Lyapunov function is defined as

$$E = \frac{1}{2}I_{\text{o}}^2 + \frac{1}{2}V_{\text{c}}^2 \tag{33}$$

where V_{c} and I_{o} are the voltage and current, respectively. To ensure the system stability, the first-time derivative of the Lyapunov function must be negative definite. Therefore, the first-time derivative of (33) can be derived as

$$\dot{E} = I_{\text{o}}\dot{I}_{\text{o}} + V_{\text{c}}\dot{V}_{\text{c}} \tag{34}$$

Then, substituting (32) into (34) yields

$$\begin{aligned}\dot{E} = {} & \boldsymbol{I}_{\text{o}}\left(-\Gamma\boldsymbol{k}_1^{-1}\boldsymbol{V}_{\text{c}} - \Gamma\boldsymbol{k}_1^{-1}\boldsymbol{R}\boldsymbol{I}_{\text{o}} - \Gamma\boldsymbol{k}_i\boldsymbol{I}_{\text{o}}^n - \Gamma\boldsymbol{I}_{\text{o}} + \Gamma\boldsymbol{k}_1^{-1}\boldsymbol{V}^*\right) \\ & + \boldsymbol{V}_{\text{c}}\left(-\boldsymbol{C}^{-1}\boldsymbol{L}_{\text{L}}\boldsymbol{V}_{\text{c}} + \boldsymbol{C}^{-1}\boldsymbol{I}_{\text{o}}\right)\end{aligned} \tag{35}$$

Finally, recalling (31) as the first derivation of the Lyapunov function can be represented as

$$\begin{aligned}\dot{E} = {} & -\Gamma\boldsymbol{k}_i\boldsymbol{I}_{\text{o}}^{n+1} - \Gamma\boldsymbol{I}_{\text{o}}^2 - \boldsymbol{C}^{-1}\boldsymbol{L}_{\text{L}}\boldsymbol{V}_{\text{c}}^2 \\ & + \frac{\boldsymbol{I}_{\text{L}i}\boldsymbol{I}_{\text{o}}}{\boldsymbol{L}_{\text{L}}}\left(\boldsymbol{C}^{-1} + \Gamma\boldsymbol{k}_1^{-1}\left(\frac{\boldsymbol{V}^* - \boldsymbol{V}_{\text{c}} + \boldsymbol{R}\boldsymbol{I}}{\boldsymbol{V}_{\text{c}}}\right)\right) \le 0\end{aligned} \tag{36}$$

It should be noted that the last term in (36) is negative since V_{c} is large enough to compensate the drop voltage due to the line impedance. Moreover, I_{o} and $I_{\text{L}i}$ are in the same direction. Therefore, from (36), it can be seen that for all odd values of n, the first-time derivation of the Lyapunov function is negative definite and the proposed control method guarantees the stability of the DCNG's cluster.

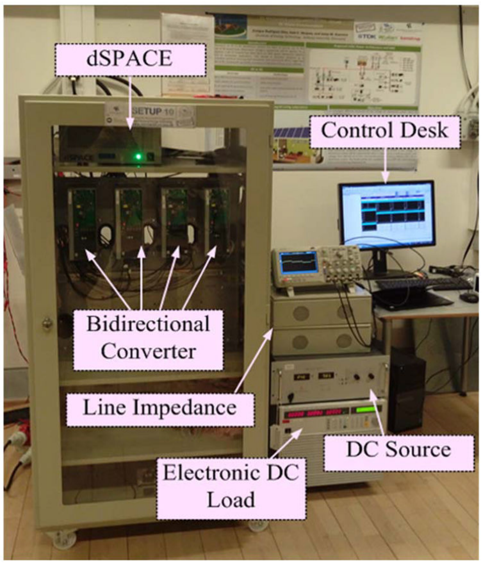

Fig. 8 *Hardware setup for experimental measurements*

Table 1 Experimental parameters

Parameters	Value
Electrical parameters	
DC bus voltage	48 V
input voltage	24 V
converter inductance	1800 μH
DC bus capacitance	8800 μF
line resistance for DCNG1	0.4 Ω
line resistance for DCNG2	0.7 Ω
line resistance for DCNG3	1.3 Ω
line resistance for DCNG4	1 Ω
Droop control parameters	
k_p	3
k_i	15
k_1	0.2

6 Experimental results

To validate the performance of the proposed method, a DCNG cluster consisting of four sources is implemented. As shown in Fig. 8, for experimental tests, a DCMG setup consists of four bidirectional converters, line impedances, resistive and constant power loads, monitoring system, and dSPACE emulator is developed. The nominal voltage for the DCNG cluster is 48 V. The electrical and control parameters are listed in Table 1. The experimental results are shown in Figs. 9–12 for different scenarios.

6.1 Heavy-loading condition

Fig. 9 shows the experimental results for a heavy-loading condition in the DCNG cluster. At $t = 1.8$ s, a common load of 1.5 kW is applied due to which the voltage in the DC bus drops from 48 to 47 V and the DCNGs starts contributing for the common load. Fig. 9*a* shows the DC bus voltage in this case study. It can be seen that the DC bus voltage remains within an acceptable range (i.e. $V_H = 49.2$ V and $V_L = 46.8$ V) with the proposed control scheme. From Fig. 9*b*, it can be seen that the current sharing among the DCMGs is realised accurately with the different line resistances. In this case, the current of each DCNG reaches about 8 A to contribute for common load on the DC bus. Moreover, Fig. 9*c* shows the power of the common load on the DC bus. It can be seen that the proposed *I*–*V* droop control has a faster transient response as well as it has a desired current sharing among the DCNGs.

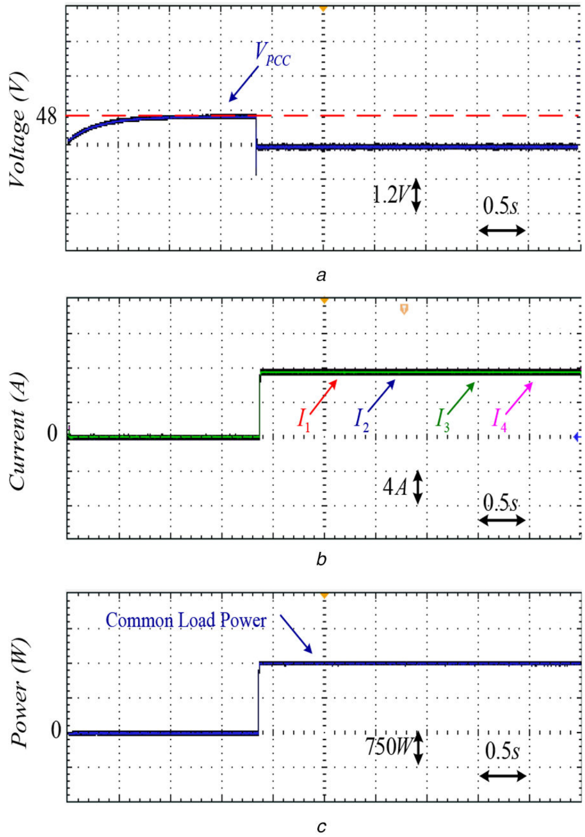

Fig. 9 *Experimental results in heavy-loading condition*
(a) DC bus voltage, ***(b)*** Current sharing among DCNGs, ***(c)*** Power of the common load in DC bus

6.2 Light-loading condition

This section illustrates the performance of the proposed method under light-loading condition. To realise the performance of the proposed control method in this condition, at $t = 1.8$ s a common load of 400 W is considered in the DC bus. From Fig. 10*a*, it can be observed that on the application of the common load, the DC bus voltage has the desired profile when the light load is connected to the DCNGs, which drops from 48 to 47.8 V. From Fig. 10*c*, it can be observed that in this situation, the proposed method guaranteed the accurate current sharing among the DCNGs in a cluster with the different line resistance. It can be concluded from Sections 6.1 and 6.2 that the proposed control method has the desired performance during all loading conditions from light to heavy load and has the maximum available droop gain in all situations to guarantee the best current sharing among the DCNGs.

6.3 Step change in load (dynamic condition)

Studies in this section illustrate the performance of the proposed method in a dynamic condition. Fig. 11 shows the experimental results during step changes in the common load for two step-up changes from 0 to 1.1 and 1.1 to 1.5 kW; moreover, a step-down changes from 1.5 to 750 W in the DC bus. It can be observed that during step load changes, the proposed method has a good transient response (Fig. 11*a*) and the whole system is stable. Moreover, in this condition, the currents of the DCNG follow the reference current properly and the accurate current sharing can be achieved with different line resistances in the DCNGs.

6.4 Connection and disconnection of the DCNGs

In this case, the performance of the system under the proposed method during connection and disconnection (i.e. plug-and-play capability) of the DCNGs to the cluster is illustrated. Here, two DCNGs (i.e. DCNG1 and DCNG2) are injected power to the common load for all the time. As shown in Fig. 12, at the beginning of the test, a common load is connected to the bus and

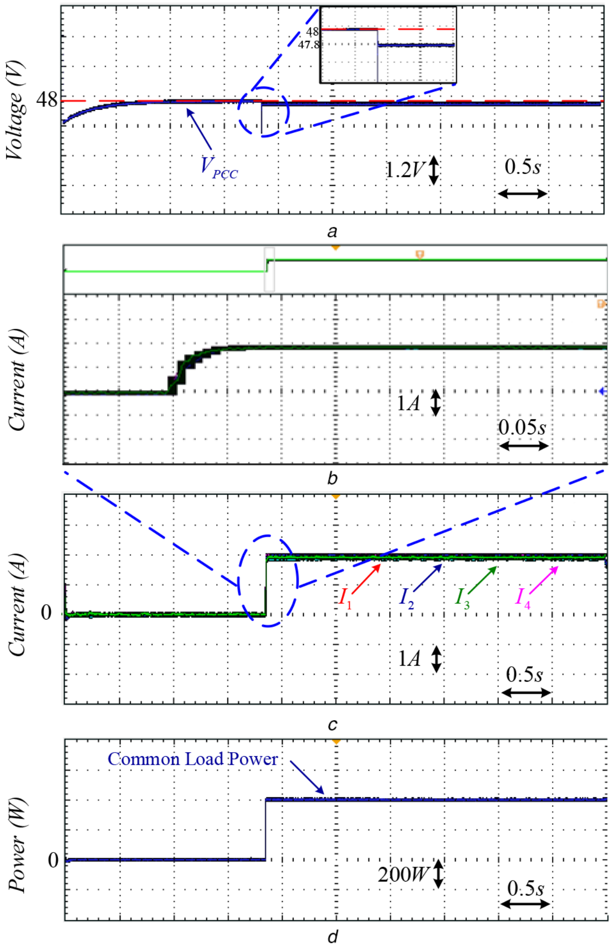

Fig. 10 *Experimental results in light-loading condition*
(a) Voltage of DC bus, ***(b)*** Transient response of currents, ***(c)*** Current sharing among DCNGs, ***(d)*** Power of the common load in DC bus

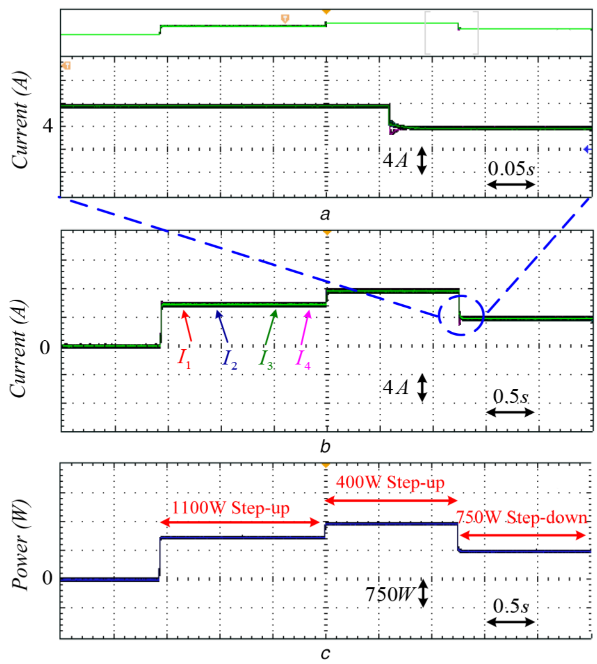

Fig. 11 *Experimental measurements in dynamic condition*
(a) Transient response of DCNG's current, ***(b)*** Current sharing among DCNGs, ***(c)*** Step changes in the common load

DCNG1 and DCNG2 share the total current equally. At $t = 0.6$ s, the DCNG3 is connected (plug-in) to the cluster and starts the injection power to the common load. As shown in Fig. 12*b*, the total load is shared between DCNGs properly. Moreover, at

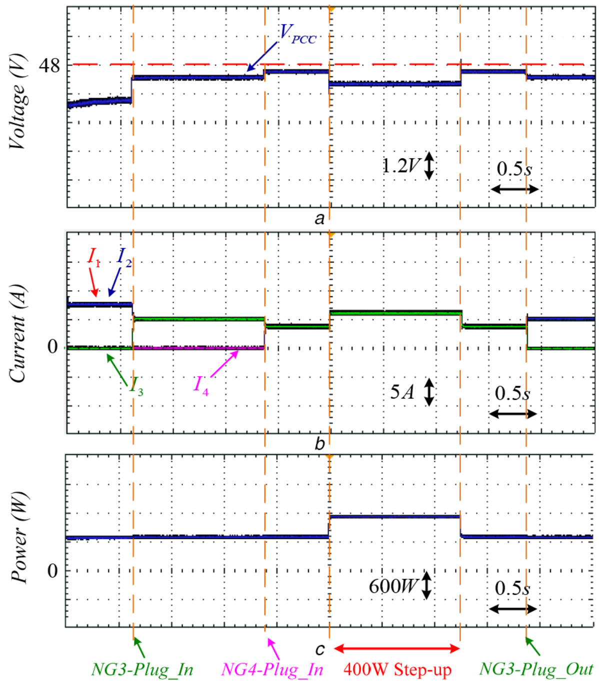

Fig. 12 *Experimental results for Plug_in and Plug_out of the DCNGs*
(a) DC bus voltage, ***(b)*** Current sharing among DCNGs, ***(c)*** Step change in the common load

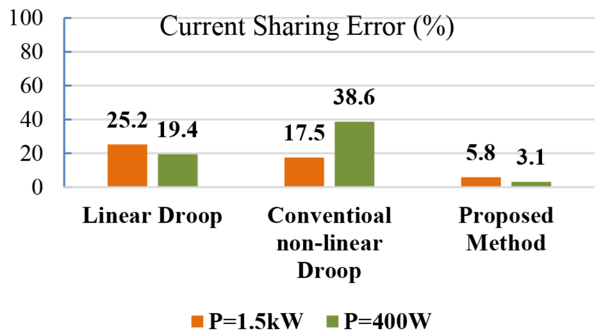

Fig. 13 *Comparison of the current-sharing error*

$t = 1.9$ s, the DCNG4 is connected to the system and all DCNGs participate in power injection to the load. It can be seen from Fig. 12*b* that the accurate current sharing among DCNGs can be guaranteed with the proposed method. To show the performance of the proposed method clearly, a step load change is applied from $t = 2.5$ to 3.75 s when all DCNGs are connected to the DC bus. From Fig. 12*b*, it can be observed that all agents share the total load current equally. Moreover, to validate the stability of the system under the proposed control method, it is assumed that the DCNG3 plugged out at $t = 4.9$ s. Consequently, due to this disconnection, the current sharing among the DCNGs is affected and three DCNGs (i.e. DCNG1, DCNG2, and DCNG4) are contributed in the common load. From Fig. 12*b*, it can be seen that the proposed control method presents proper performance during connection and disconnection of the DCNGs. As shown in Fig. 12*a*, in all transient conditions, the stability of the DC bus voltage can be guaranteed as well as the voltage regulation in steady state.

Fig. 13 shows the current-sharing performance comparison of the conventional methods and the proposed method. Fig. 13 also shows the difference of the proposed method over other controllers. From Fig. 13, it can be concluded that linear droop method offers good current sharing in the light-load condition. It is also seen that the conventional non-linear droop control methods offer good current-sharing performance in the heavy-load condition. However, its current-sharing accuracy is not as good as the linear droop technique at the light-load conditions. Fig. 13 shows the proposed method provides the best current sharing among all the methods from the light-load to full-load condition. Therefore, the current-sharing performance is better than the other two techniques. In summary, it is observed that the proposed method enhances the current-sharing accuracy for a given voltage deviation.

7 Conclusion

In this paper, a non-linear *I–V* droop control was presented. The current sharing and voltage regulation of the DCNGs in a cluster with consideration of the effect of line impedance were analysed. It was presented that with the fully decentralised proposed control method, the current sharing among the DCNGs was enhanced and the voltage regulation was achieved as well as the plug-and-play capability was implemented, which provides scalability and modularity for the DCNGs in a cluster. The stability analysis was carried out to investigate the performance of the proposed method. The effectiveness of the proposed method was presented with experimental tests in several conditions (i.e. light- and heavy-loading conditions, step load change, and connection/disconnection of DCNGs). It can be concluded that the proposed method has a faster response during transient and enhanced current sharing among DCNGs. For the future works, the researchers can investigate on the high-performance energy management methods for the DCNGs.

8 References

[1] Rocabert, J., Luna, A., Blaabjerg, F.*, et al.*: 'Control of power converters in AC microgrids', *IEEE Trans. Power Electron.*, 2012, **27**, (11), pp. 4734–4749

[2] Nasir, M., Jin, Z., Khan, H.*, et al.*: 'A decentralized control architecture applied to DC nanogrid clusters for rural electrification in developing regions', *IEEE Trans. Power Electron.*, 2019, **34**, pp. 1773–1785

[3] Shahidehpour, M., Li, Z., Gong, W.*, et al.*: 'A hybrid ac/dc nanogrid: the Keating Hall installation at the Illinois Institute of Technology', *IEEE Electrification Mag.*, 2017, **5**, (2), pp. 36–46

[4] Sun, K., Wang, X., Li, Y.W.*, et al.*: 'Parallel operation of bidirectional interfacing converters in a hybrid AC/DC microgrid under unbalanced grid voltage conditions', *IEEE Trans. Power Electron.*, 2017, **32**, (3), pp. 1872–1884

[5] Shafiee, Q., Dragičević, T., Vasquez, J.C.*, et al.*: 'Hierarchical control for multiple DC-microgrids clusters', *IEEE Trans. Energy Convers.*, 2014, **29**, (4), pp. 922–933

[6] Abdelaziz, M.M.A., Shaaban, M.F., Farag, H.E.*, et al.*: 'A multistage centralized control scheme for islanded microgrids with PEVs', *IEEE Trans. Sustain. Energy*, 2014, **5**, (3), pp. 927–937

[7] Meng, L., Dragicevic, T., Roldán-Pérez, J.*, et al.*: 'Modeling and sensitivity study of consensus algorithm-based distributed hierarchical control for DC microgrids', *IEEE Trans. Smart Grid*, 2016, **7**, (3), pp. 1504–1515

[8] Schiffer, J., Seel, T., Raisch, J.*, et al.*: 'Voltage stability and reactive power sharing in inverter-based microgrids with consensus-based distributed voltage control', *IEEE Trans. Control Syst. Technol.*, 2016, **24**, (1), pp. 96–109

[9] Guerrero, J.M., Vasquez, J.C., Matas, J.*, et al.*: 'Hierarchical control of droop-controlled AC and DC microgrids – a general approach toward standardization', *IEEE Trans. Ind. Electron.*, 2011, **58**, (1), pp. 158–172

[10] Kumar, M., Srivastava, S.C., Singh, S.N.: 'Control strategies of a DC microgrid for grid connected and islanded operations', *IEEE Trans. Smart Grid*, 2015, **6**, (4), pp. 1588–1601

[11] Wang, P., Lu, X., Yang, X.*, et al.*: 'An improved distributed secondary control method for DC microgrids with enhanced dynamic current sharing performance', *IEEE Trans. Power Electron.*, 2016, **31**, (9), pp. 6658–6673

[12] Peyghami, S., Mokhtari, H., Loh, P.C.*, et al.*: 'Distributed primary and secondary power sharing in a droop-controlled LVDC microgrid with merged AC and DC characteristics', *IEEE Trans. Smart Grid*, 2018, **9**, (3), pp. 2284–2294

[13] Nasirian, V., Davoudi, A., Lewis, F.L.*, et al.*: 'Distributed adaptive droop control for DC distribution systems', *IEEE Trans. Energy Convers.*, 2014, **29**, (4), pp. 944–956

[14] Zhao, X., Li, Y.W., Tian, H.*, et al.*: 'Energy management strategy of multiple supercapacitors in a DC microgrid using adaptive virtual impedance', *IEEE J. Emerg. Sel. Top. Power Electron.*, 2016, **4**, (4), pp. 1174–1185

[15] Hu, J., Duan, J., Ma, H.*, et al.*: 'Distributed adaptive droop control for optimal power dispatch in DC microgrid', *IEEE Trans. Ind. Electron.*, 2018, **65**, (1), pp. 778–789

[16] Lu, X., Sun, K., Guerrero, J.M.*, et al.*: 'State-of-charge balance using adaptive droop control for distributed energy storage systems in DC microgrid applications', *IEEE Trans. Ind. Electron.*, 2014, **61**, (6), pp. 2804–2815

[17] Dragicevic, T., Guerrero, J.M., Vasquez, J.C.*, et al.*: 'Supervisory control of an adaptive-droop regulated DC microgrid with battery management capability', *IEEE Trans. Power Electron.*, 2014, **29**, (2), pp. 695–706

[18] Lu, L.Y., Chu, C.C.: 'Consensus-based droop control synthesis for multiple DICs in isolated micro-grids', *IEEE Trans. Power Syst.*, 2015, **30**, (5), pp. 2243–2256

[19] Lu, L.Y., Chu, C.C.: 'Consensus-based secondary frequency and voltage droop control of virtual synchronous generators for isolated AC micro-grids', *IEEE J. Emerg. Sel. Top. Circuits Syst.*, 2015, **5**, (3), pp. 443–455

[20] Guan, Y., Meng, L., Li, C.*, et al.*: 'A dynamic consensus algorithm to adjust virtual impedance loops for discharge rate balancing of AC microgrid energy storage units', *IEEE Trans. Smart Grid*, 2018, **9**, (5), pp. 4847–4860

[21] Lu, X., Guerrero, J.M., Sun, K.*, et al.*: 'An improved droop control method for DC microgrids based on low bandwidth communication with DC bus voltage restoration and enhanced current sharing accuracy', *IEEE Trans. Power Electron.*, 2014, **29**, (4), pp. 1800–1812

[22] Moayedi, S., Davoudi, A.: 'Distributed tertiary control of DC microgrid clusters', *IEEE Trans. Power Electron.*, 2016, **31**, (2), pp. 1717–1733

[23] Peyghami, S., Mokhtari, H., Blaabjerg, F.: 'Decentralized load sharing in a low-voltage direct current microgrid with an adaptive droop approach based on a superimposed frequency', *IEEE J. Emerg. Sel. Top. Power Electron.*, 2017, **5**, (3), pp. 1205–1215

[24] Wang, C., Duan, J., Fan, B.*, et al.*: 'Decentralized high-performance control of DC microgrids', *IEEE Trans. Smart Grid*, 2019, **10**, (3), pp. 3355–3363

[25] Wang, H., Han, M., Han, R.*, et al.*: 'A decentralized current-sharing controller endows fast transient response to parallel DC–DC converters', *IEEE Trans. Power Electron.*, 2018, **33**, (5), pp. 4362–4372

[26] Prabhakaran, P., Goyal, Y., Agarwal, V.: 'Novel nonlinear droop control techniques to overcome the load sharing and voltage regulation issues in DC microgrid', *IEEE Trans. Power Electron.*, 2018, **33**, (5), pp. 4477–4487

[27] Chen, F., Burgos, R., Boroyevich, D.*, et al.*: 'Investigation of nonlinear droop control in DC power distribution systems: load sharing, voltage regulation, efficiency and stability', *IEEE Trans. Power Electron.*, 2019, **34**, (10), pp. 9404–9421

[28] Han, R., Meng, L., Guerrero, J.M.*, et al.*: 'Distributed nonlinear control with event-triggered communication to achieve current-sharing and voltage regulation in DC microgrids', *IEEE Trans. Power Electron.*, 2018, **33**, (7), pp. 6416–6433